Journal of Al-Azhar University Engineering Sector

Vol.18, No. 69, October 2023, 998- 1008

The Potential of Multispectral Lidar for Building Extraction in a Complex Urban Area Using CANUPO Algorithm

Asmaa. A. Mandouh[1*], Mahmoud E.O. Ali[2], Mostafa H. A. Mohamed[2], Lamyaa G. E. Taha[1]

[1] Division of Aerial Photography and Aviation, National Authority for Remote Sensing and Space Sciences, Cairo, Egypt.
[2]Civil Engineering Department, Faculty of Engineering, Al-Azhar University, Cairo, Egypt.
* Correspondence: asmaa..ahmed@narss.sci.eg

Citation:

A. A. Mandouh, M. E. O. Ali, M.H.A. Mohamed, L.G.E.Taha "The Potential of Multispectral Lidar for Building Extraction in a Complex Urban Area Using CANUPO Algorithm", Journal of Al-Azhar University Engineering Sector, vol. 18, pp. 998-1008, 2023.

Received: 28 May 2023

Accepted: 15 July 2023

DoI:10.21608/auej.2023.213893.1376

ABSTRACT

The process of extracting buildings from remotely sensed data is essential for various applications such as 3D building modeling, city planning, disaster evaluation, and updating digital maps and GIS databases. The primary focus of this study is to examine how well multi-spectral lidar can extract individual buildings in dense urban environments. Recently developed remote sensing technologies include multi-spectral lidar. The primary lidar only uses one wavelength (NIR), while this newer gadget combines three wavelengths (NIR, MID, and Green) for more comprehensive data. This study evaluated multi-spectral lidar's effectiveness in extracting buildings from metropolitan regions under two different scenarios. The first scenario, which is a simplification of the single-wavelength lidar, utilized the initial return from the NIR alone. Since each wavelength of multispectral lidar contains four numbers of returns, they were combined to form a single dataset for the second scenario. The data underwent a filtration process to distinguish between ground and non-ground points, enhancing the building extraction's efficacy in both scenarios. The two scenarios in the CANUPO algorithm were executed using open-source software cloud-compare. This method utilizes multiscale dimensions to attain high-quality results while ensuring ground objects' safety. Eigenvalues were computed for all data points using varying scales ranging from 10m to 100m. The findings indicate that the second scenario, utilizing the spectral diversity of multispectral lidar for more efficient extraction of building points compared to the first scenario, resulted in a 95% improvement in balanced accuracy.

KEYWORDS: Multispectral Lidar, Point Cloud, CANUPO, Building Extraction, Lidar.

إمكانات الليدار متعدد الأطياف لاستخراج المباني في منطقة حضرية معقدة باستخدام خوارزمية كانبو

أسماء أحمد مندوه[1*] ، محمود النقراشي عثمان علي [2] ، مصطفي حسن عبد الستار [2] ، لمياء جمال الدين طه [1]

[1] شعبه التصوير الجوي والطيران، الهيئه القوميه للاستشعار من البعد وعلوم الفضاء ، القاهره، مصر
[2]قسم الهندسة المدنية، كلية الهندسة ، جامعة الازهر ، القاهره، مصر
***البريد الاليكتروني للباحث الرئيسي:** asmaa.ahmed@narss.sci.eg

الملخص

عملية استخراج المباني من بيانات الاستشعار عن بعد ضرورية للعديد من التطبيقات مثل نمذجة المباني ثلاثية الأبعاد ، وتخطيط المدن ، وتقييم الكوارث ، وتحديث الخرائط الرقمية وقواعد بيانات نظم المعلومات الجغرافية. ينصب التركيز الأساسي لهذه الدراسة على دراسة مدى قدرة الليدار متعدد الأطياف على استخراج المباني الفردية من البيئات الحضرية الكثيفة. تشتمل تقنيات الاستشعار عن بعد المطورة حديثًا على الليدار متعدد الأطياف. يستخدم الليدار الأساسي طولًا موجيًا واحدًا فقط (NIR) ، بينما تجمع هذه الأداة الأحدث ثلاثة أطوال موجية (NIR و MID والأخضر) للحصول على بيانات أكثر شمولاً.

قيمت هذه الدراسة فعالية الليدار متعدد الأطياف في استخراج المباني من المناطق الحضرية في إطار سيناريوهين مختلفين. استخدم السيناريو الأول ، وهو تبسيط ليدار أحادي الطول الموجي ، العائد الأولي من NIR وحده. نظرًا لأن كل طول موجي لليدار متعدد الأطياف يحتوي على أربعة أعداد من المرتجعات ، فقد تم دمجها لتشكيل مجموعة بيانات واحدة للسيناريو الثاني. خضعت البيانات لعملية تنقيه للتمييز بين النقاط الأرضية وغير الأرضية ، وبالتالي تعزيز فعالية استخراج المباني في كلا السيناريوهين. تم تنفيذ السيناريوهين في خوارزمية CANUPO المتوفره في برنامج مجاني مفتوح المصدر. تستخدم هذه الطريقة أبعادًا متعددة النطاقات لتحقيق نتائج عالية الجوده. تم حساب القيم الذاتية لجميع نقاط البيانات باستخدام مقاييس ثبات مختلفة تتراوح من 10m إلى 100m. تشير النتائج إلى أن السيناريو الثاني ، باستخدام التنوع الطيفي لليدار متعدد الأطياف لاستخراج نقاط بناء أكثر كفاءة مقارنةً بالسيناريو الأول ، أدى إلى تحسن بنسبة 95٪ في الدقة الكلية (OA).

الكلمات المفتاحية : الليدار متعدد الاطياف, النقاط السحابيه, الليدار, استخراج المباني , كانبو لوغاريتم

1. INTRODUCTION

3D laser scanning is a high-efficiency method for the capture of data. It is rapidly maturing technology and continuously falling costs will provide ideal data support for the creation of digital cities in the future. The development of digital cities relies on a comprehensive, true, and accurate representation of geographical entities and the information related to their environments. This representation is also one of the primary research challenges that pertain to 3D GIS. The reflection intensity that is produced by the three-dimensional laser is an important aspect of laser scanning, and even in conditions with low levels of ambient light, it is still possible to identify the target to some degree using this technique [1-3].

Titan was the first multispectral lidar system to be released by the Teledyne Optic company in Ontario, Canada, in 2014 [4]. Since then, Titan has demonstrated its superiority over single-wavelength lidar in numerous applications related to remote sensing, particularly feature extraction and accurate classification. It is now possible, thanks to the multispectral Lidar system, to obtain the geometric and spectral information of the ground features faster and accurately at the same time without data fusion. This is because of the system's ability to collect information in multiple spectral bands [5]. Multispectral lidar also offers four Number Of Returns (NOR) instead of the one return provided by single-wavelength lidar. The interplay of each feature with various wavelengths (such as reflection off the water surface and/or aqueous benthic layer, and greening of vegetation) is responsible for the variation in the number of returns across channels [6]. This system operates with three channels at different angles to acquire three-point clouds. These channels are as follows: channel -1 at mid-infrared (MIR) with a wavelength of 1550 nm at 3.5° forward-looking; channel -2 at near-infrared (NIR) with a wavelength of 1064 nm at 0° nadirs looking; and channel -3 at Green with a wavelength of 532 nm at 7° forward-looking [7]. Point clouds from three different wavelength accords have higher accuracy and precision compared with mono-wavelength point clouds [8].

Numerous studies have examined the extraction of buildings from single-wavelength lidar data. Previous studies typically employed the conversion of raw lidar points into raster images as an initial step in the building extraction process [9, 10]. Cloud point data is utilized to obtain elevation and intensity information [11,12]. However, this results in a reduction of geographic information, thereby adversely impacting the quality of data processing. With advancements in computation, certain researchers have found it appealing to directly process lidar point clouds without the need for rasterization procedures [13-15].

In recent years, several studies have focused on the utilization of deep learning and machine learning models to extract buildings from lidar data. These studies include the works of [16-20]. [21] have made progress in the field of building extraction from lidar data. However, a challenge remains in directly extracting buildings from the raw lidar point cloud directly due to the irregularity of the cloud points and the large volume of data, in addition to the lack of proliferation of deep learning networks that deal with those points directly and such methods need specialized people in machine learning. [22] developed the CANUPO suite designed to manage extensive point cloud datasets in cloud-computing environments. This tool facilitates the automated utilization by individuals without expertise in machine learning, while also providing straightforward management of the classification process. Consequently, the CANUPO algorithm was utilized to extract buildings from a multispectral lidar point cloud which is based on multi-scale dimensions. This was done through two scenarios: the first scenario relied solely on the wavelength of the first channel (NIR) as a representation of the single-wavelength lidar, while the second scenario integrated the three wavelengths, to investigate the comparative efficacy of single-wavelength lidar and multispectral lidar in the extraction of buildings from complex urban areas.

2. Study Area and Dataset

Study Area

Research data were obtained from a sample dataset provided by the Hyperspectral Image Analysis Laboratory and the National Center for Airborne Laser Mapping (NCALM) at the University of Houston. The dataset relates to the city of Houston located in the southeastern region of Texas, USA. The research area includes the University of Houston campus and surrounding areas. Fig. 1. depicts an aerial photograph of the study area, incorporating various land cover elements such as buildings, roads, asphalt parking lots, trees, grass, cars, and electric power wires. Our research focuses on identifying and extracting buildings from a complex urban environment comparable to the study area, which is characterized by varying degrees of roof structure complexity. The area contains both conventional and nonconventional structures, such as buildings with intricate designs and varied dimensions. This area also contains a combination of low-rise and high-rise structures.

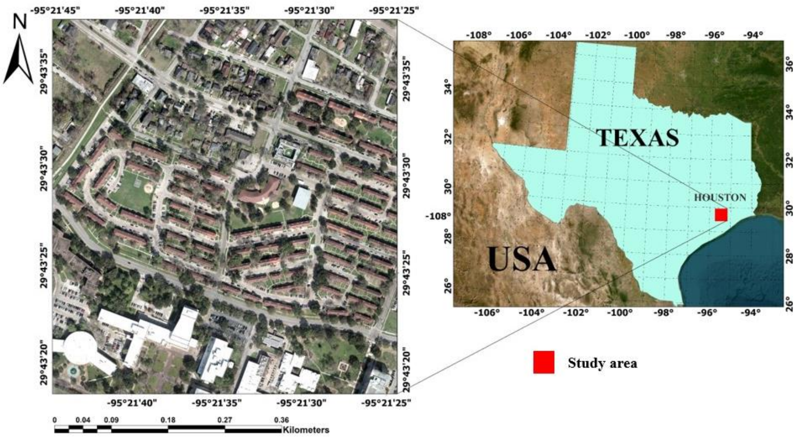

Fig. 1: Study area.

A 600 m by 600 m subset of lidar data was clipped for the experimental testing. **Table 1** summarizes the parameters coordinates of the dataset and **Table 2** shows the specifications of the data subset. The average point spacing is defined as the average distance between two adjacent points within a single point cloud, the average point density describes the number of points per m² in the study area.

Table 1: Study area geospatial reference summary.

Parameters	Specifications
Project description	UTM Zone 15 / NAD83
Project datum	NAD83
Project unit	meters
Upper left (X, Y)	271460.000, 3290890.990
Lower right (X, Y)	272055.990, 3290290.000

Table 2: Parameters of the cropped and merged data.

parameters	CH-1 (NIR)	CH-2 (MID)	CH-3 (GREEN)
Lidar point count	1,655,457	1,424,207	1,444,933
Lidar point density	5.476 samples/m²	4.765 samples/m²	5.016 samples/m²
Lidar point spacing	0.4273m	0.4581 m	0.4465 m

DATASET

The research region was scanned in February 2017 using a Teledyne Optech Titan multi-spectral ALS system [23]. All three spectral channels of the Titan system simultaneously collected data. Each channel has its own set of features, resulting in a comprehensive topographical presentation. The ALS dataset included multispectral data from 14 flight lines. All collected points were separately recorded in 42 lidar Aerial Survey (LAS) files, each corresponding to a distinct channel and strip. Every LAS file contained data on the point source ID, scan angle rank, flight line edge, scan direction flag, returns, GPS time, and intensity values. The full characteristics of multispectral lidar datasets are given in **Table 3**; the Titan sensor was put in an Optech aircraft that traveled at 140 knots at a height of approximately 460 meters above ground level.

Table 3: Specifications of Optech Titan multi-spectral ALS Lidar [24].

parameter	Channel 1	Channel 2	Channel 3
Wavelength	1550 nm MIR	1064 nm NIR	532 nm Green
Beam divergence	0.35 mrad(1/e)	0.35 mrad(1/e)	0.70 mrad(1/e)
Look angle	3.5 ° forward	nadir	7.0 ° forward
Effective PRF	50–300 kHz	50–300 kHz	50–300 kHz
Operating altitudes	Topographic: 300–2000 m AGL, all channels		
Scan angle (FOV)	Programmable; 0–60° maximum		
Intensity captures	Up to 4 range measurements for each pulse, including the12 bit dynamic measurement and date range		

3. METHODOLOGY

The preliminary stages of multispectral lidar data pre-processing encompass two key steps: noise elimination, and data filtering. Before implementing two distinct scenarios and inputting data into the CANUPO algorithm, which is accountable for extracting buildings from multispectral lidar points in this study, these phases are deemed essential.

Noise Elimination

The methodology employed in this study entailed the utilization of the statistical outlier removal (SOR) algorithm to eliminate isolated points or any points that fell outside the intensity range [25], which is readily accessible through the open-source Cloud Compare software. The filter was employed to remove singular point clouds and anomalous data points from LAS files for all three channels. As per the aforementioned filter, the computation involves the determination of the number of points utilized to ascertain the mean distance approximations. In the present scenario, this value was established as 6. Consequently, data points that surpass the threshold are eliminated.

Data Filtering

The Cloth Simulation Filter (CSF) provided by [26] was utilized to remove ground objects in our investigation. CSF filtering algorithm requires a few easily-adjusted logical parameters. The proposed solution comprises covering a lidar point cloud with mesh. Examining the interactions between fabric nodes and lidar points helps simulate the ground surface. The produced surface can be compared to the original lidar points to find the ground points in the point cloud. The fabric simulation filter has advanced options for integrating all three channels' point clouds. First, determine the ground cloth's grid size, 0.5, 500 iterations for terrain simulation are required. We set the Classification threshold to 0.5 to classify point clouds by distance. Considering the area's flat terrain.

Training data / Dimensional features at multiple scales

The CANUPO algorithm is a semi-supervised learning, was developed by [22]. The algorithm has been integrated into the Cloud Compare V2.13 plugin toolbar. The CANUPO algorithm possesses the benefit of semi-automatically categorizing clouds. The implementation of 3D rasterization without the utilization of a rasterization phase. Furthermore, it is possible to create personalized classifiers by subjecting them to limited datasets and subsequently sequentially implementing them across the complete point cloud to categorize them into the intended classes. In addition, the system furnishes a confidence value that is labeled for every point, thereby facilitating the identification of outliers, particularly at the boundaries of classes. The goal of this classification technique is to identify the optimal dimensionality measurement scales that will allow for optimal separation between two or more classes [22]. The present study focuses on the application of the CANUPO algorithm for building extraction. The study includes an analysis of classification outcomes at various scales ranging from 10 m to 100 m. The objective is to identify the optimal scale for building extraction with maximum precision. The study further extends to the application of the identified scale to a residential area that encompasses multiple building models. Exemplary classification results are presented for reference. Furthermore, the identical classification algorithm utilizing multiple scales was employed in the initial scenario to depict single-wavelength lidar, as well as in the second scenario to represent lidar, and subsequently, the outcomes were assessed.

4. Results and Discussion

4.1 CANUPO Results for Using CH-1

The scope of this scenario was restricted to the assessment of the CH-1, which serves as a single-wavelength lidar technology utilized for building extraction. The utilization of the CSF algorithm enabled the segregation of ground points from non-ground points, thereby facilitating the extraction of buildings. The results of the CSF filtering process for CH-1 are presented in Fig. 2. The raw point cloud data for CH-1, which is depicted in Fig. (2a), consists of a total of 1,655,457 points. After the implementation of the CSF filtering algorithm, the non-ground points amount to 779,568, as depicted in Fig. (2b). On the other hand, Figure 3c illustrates that there are 875,889 points on the ground.

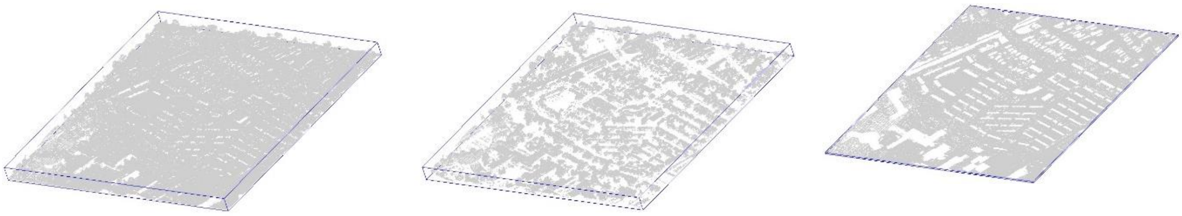

(a) (b) (c)

Fig. 2: Results of CSF filtering for CH-1: (a) raw point cloud of CH-1, (b) off-ground point cloud of CH-1, (c) ground point cloud for ch-1.

Following pre-processing techniques applied to the lidar data obtained from channel -1, a CANUPO logarithm was utilized in conjunction with multiscale combinations of building dimensions. This methodology aims to instruct a logarithmic function to precisely recognize buildings. Fig. 3 displays the outcomes of the CANUPO algorithm implemented at various scales. The study was conducted utilizing scales ranging from 10 to 100 meters, with an incremental increase of 10 meters per iteration. The experiment commenced at a distance of 10 meters, as depicted in Fig. (3a). Subsequently, the scale was incremented by 10 meters in each trial until it reached a distance of 100 meters, as illustrated in Fig. (3j).

As depicted in Fig. 3, the results demonstrated that the logarithm could not be effectively trained to recognize buildings using a 10-meter scale. In addition, as the scale increases, the density of correctly classified building point clouds increases, as does the ability to correctly recognize and identify buildings through the application of the logarithm. As demonstrated by the previous experiment utilizing a scale of 100 meters, the results of building extraction were enhanced. It is also evident that small buildings were recognized by tiny scales, whereas as the scale increased, the logarithm recognized large buildings. Consequently, it is justifiable to consider building dimensions and use a scale that can accommodate the greatest building size in the study area.

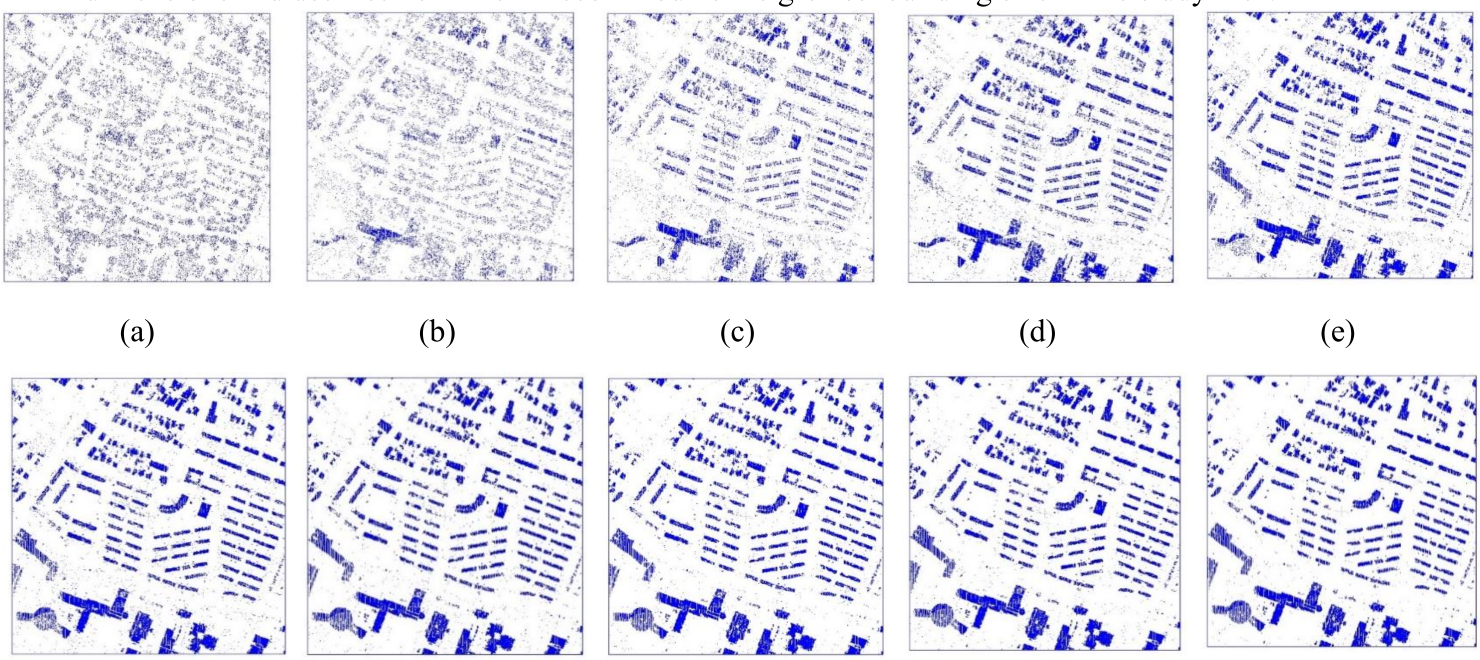

(a) (b) (c) (d) (e)

(f) (g) (h) (i) (j)

Fig. 3: Results of CANUPO for using CH-1 with multi-scales: (a) with 10m, (b) with 20m, (c) with30, (d) with 40m, (e)with 50m, (f) with 60m, (g) with 70m, (h) with 80m, (i) with 90m, (j) with 100m, where blue is referred to building point cloud, and gray is referred to non- building point cloud.

4.2 CANUPO Results for Using All Merged Multispectral Lidar Channels

Using the three wavelengths, the total number of points is 4,524,597 as shown in Fig. (4a). After applying the CSF filtering algorithm, the number of non-ground points is 1,829,697 as shown in Fig.(4b), and there are 2,694,900 points on the ground as shown in Fig. (4c).

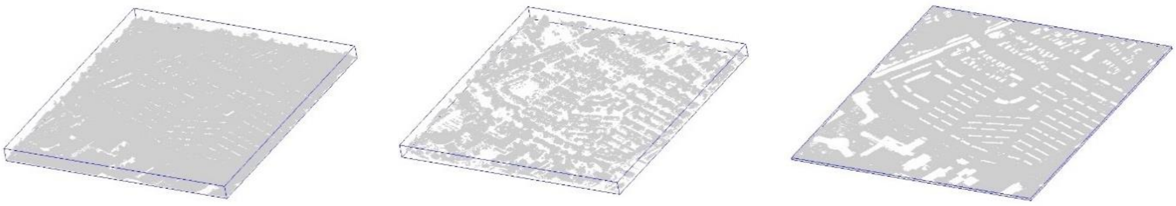

(a) (b) (c)

Fig. 4: Results of CSF filtering for all merged multispectral lidar channels: (a) raw point cloud after merging three channels, (b) non-ground point cloud, (c) ground point cloud.

The point cloud for building extraction depicted in Fig. 5 was acquired through the integration of all three channels of multispectral lidar data. After that, the CANUPO algorithm was implemented on ten distinct sets of metrics, with each set commencing at a distance of 10 meters and progressing in increments of 10 meters until reaching a maximum distance of 100 meters. Similar to the initial scenario. The point cloud feature extraction process depicted in Fig. (5j) involved the utilization of a classifier and a scale of 100 meters to attain the most effective differentiation between buildings and non-buildings.

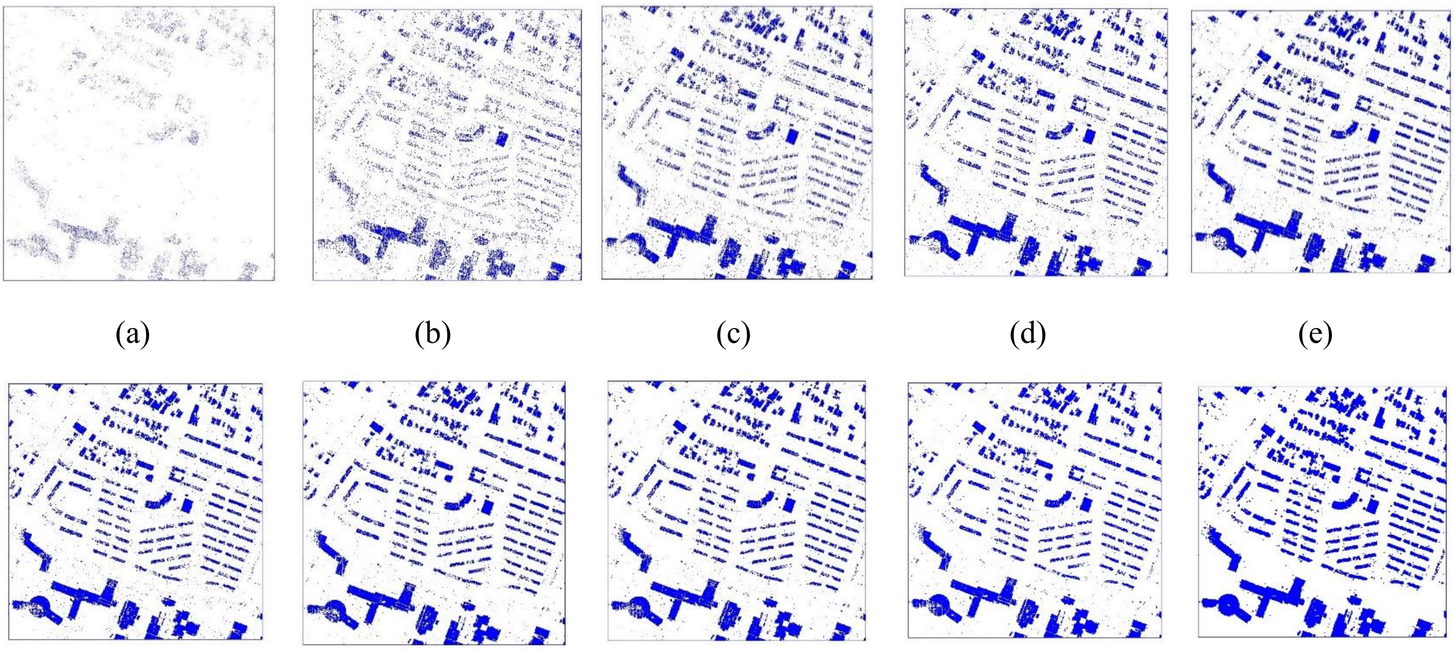

(a) (b) (c) (d) (e)

(f) (g) (h) (i) (j)

Fig. 5: Results of CANUPO for using all multispectral lidar channels with multi-scales: (a) with 10m, (b) with 20m, (c) with30, (d) with 40m, (e)with 50m, (f) with 60m, (g) with 70m, (h) with 80m, (i) with 90m, (j) with 100m, where blue is referred to the building point cloud, and gray is referred to non- building point cloud.

The optimal identification of buildings of all sizes in the study area was achieved through an increase in scale. In the second scenario, there was a notable distinction between buildings and vegetation, which was not the case in the first scenario. The latter exhibited difficulty in accurately distinguishing certain buildings, particularly those that were obscured by foliage. The reason for this can be attributed to the differentiation of multi-spectral lidar based on point density. The amalgamation of three wavelengths in multi-spectral lidar yields superior outcomes in comparison to single-wavelength lidar in terms of identifying buildings in urban areas, resulting in a higher level of accuracy.

To quantitatively assess the efficacy of each building extraction scale in the two scenarios delineated in this investigation, a balanced accuracy scale (ba) was employed [22] as follows in equations (1,2, and 3). Where are t_b ; t_n ; f_b ; f_n the number of points truly(t), and falsely(f) classified into the buildings(b)/non-building (n) classes, where a_b is the accuracy of the building class, and a_n is the accuracy of the non-building class.

$$ba = (a_b + a_n)/2 \qquad (1)$$

where,

$$a_b = \frac{t_b}{t_b + f_n} \qquad (2)$$

, and

$$a_n = \frac{t_n}{t_n + f_b} \qquad (3)$$

Table 4: Balanced accuracy scales for building extraction in two scenarios with different scales from (10-100m).

ba/ scales (m)	10	20	30	40	50	60	70	80	90	100
Scenario 1	%51.9	%75.9	%78.3	%83.7	%84.6	%87.9	%87.8	%87.8	%91.9	%92.6
Scenario 2	%81.9	%85.8	%87.5	%88.0	%90.5	%91.9	%92.3	%93.5	%95.0	%95.9

In **Table 4**, ten different groups of metrics are given. Starting from 10 meters to 100 meters in both scenarios. The higher the density of the scales, the greater the degree of increase. As the number of scales increases, the scale weights are more evenly distributed, resulting in better division. So, a higher maximum scale yields a more accurate building extraction result, but doing so requires a larger computational investment. We can conclude that multi-scale dimensional with threshold segmentation can complete the extraction of buildings and is used to ensure the integrity of building data and provide good data support for the urban modeling of digital cities. However, this process still has many shortcomings. CANUPO is not a magic tool: if the features you want to separate don’t have a clear geometrical difference, it will not work like an unclassified point cloud.

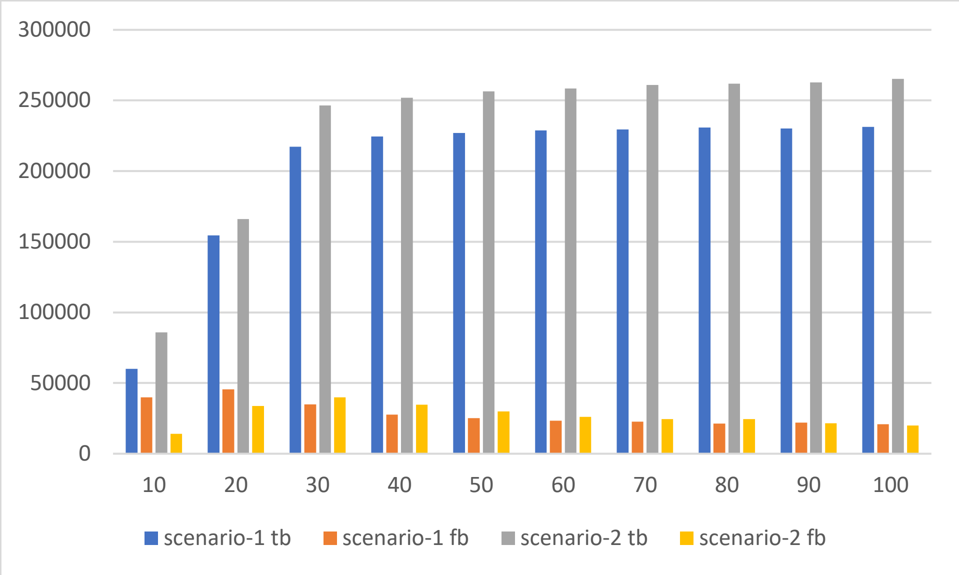

Fig. 6: Results of truly represented points for building and false points in two scenarios with different scales from 10m to 100m using the CANUPO algorithm where the t_b; t_n the number of points truly classified into buildings in two scenarios.

Fig. 6 depicts a graph illustrating the truly classified points as buildings, as well as the false classification of points as buildings, in two scenarios. The graph utilizes multiscale ranging from 10 meters to 100 meters, employing the CANUPO logarithm. The second scenario demonstrated superior performance compared to the first scenario in correctly classifying points as buildings. The second scenario exhibits a lower number of misclassified points for buildings compared to the first scenario. The use of three wavelengths yielded better results compared to the use of a single-wavelength lidar. This finding is very interesting and raises the possibility of exploring different wavelengths of building extraction using lidar in future experiments. There are a few reasons why using multiple wavelengths can improve building extraction. First, different materials reflect light differently at different wavelengths. This means that by using multiple wavelengths, we can better distinguish between different materials, such as buildings, plants, and soil. Second, the spectral signature of a building can vary depending on the building materials and conditions. By using multiple wavelengths, we can capture this difference and improve the accuracy of extracting buildings. In addition, it is recommended that future research endeavors include a comparative analysis of the CANUPO algorithm with alternative machine learning methods and traditional methods. This will serve to validate the robustness and efficacy of the aforementioned algorithm in accurately extracting buildings and other pertinent features from multispectral lidar data.

Conclusion

The present study elucidates the methodology of extracting three-dimensional (3D) buildings from multispectral point clouds utilizing the CANUPO algorithm provided by Cloud Compare, an open-source software, through multiscale feature analysis. The CANUPO algorithm is a semi-supervised classifier that facilitates the classification of three-dimensional point clouds without the need for rasterization. Moreover, it provides a classified trust value for each point, making it easy to spot outliers, especially at the category boundaries, thereby simplifying the process of distinguishing between overlapping categories. The algorithm was previously applied to plants featuring diminutive scales; however, the present study examines its efficacy in the context of extracting buildings. The process of extracting buildings was successfully executed at various scales, and a training approach was employed to identify the most effective combination of scales for accurately discriminating the point cloud of buildings from other features. The algorithm was implemented in two distinct scenarios, one of which pertains to single-wavelength lidar, while the other pertains to multi-spectral lidar. The study's findings indicate that multi-spectral lidar is a highly effective method for extracting buildings due to its ability to integrate spectral features from three distinct wavelengths (near-infrared, mid-infrared, and green). Additionally, the high point density of this technology enables the logarithm to perform optimally, resulting in more precise and accurate outcomes.

Acknowledgment: The authors thank the Hyperspectral Image Analysis Lab and the National Center for Airborne Laser Mapping (NCALM) at the University of Houston for providing the original Optech Titan data.

References

[1] Wang, R., Peethambaran, J., & Chen, D. (2018). Lidar Point Clouds to 3-D Urban Models: A Review. IEEE Journal of Selected Topics in Applied Earth Observations and Remote Sensing, 11(2).

[2] Guiotte, F., Pham, M. T., Dambreville, R., Corpetti, T., & Lefevre, S. (2020). Semantic Segmentation of Lidar Points Clouds: Rasterization Beyond Digital Elevation Models. IEEE Geoscience and Remote Sensing Letters, 17(11), 2016-2019.

[3] Song, W., Li, D., Sun, S., Zhang, L., Xin, Y., Sung, Y., & Choi, R. (2022). 2D&3DHNet for 3D Object Classification in Lidar Point Cloud. Remote Sensing, 14(13), 3146.

[4] Fernandez-Diaz, J. C., Carter, W. E., Glennie, C., Shrestha, R. L., Pan, Z., Ekhtari, N., ... & Sartori, M. (2016). Capability Assessment and Performance Metrics for The Titan Multispectral Mapping Lidar. Remote Sensing, 8(11), 936.

[5] Mahmoud El Nokrashy, O. A., Taha, L. G. E. D., Mohamed, M. H., & Mandouh, A. A. (2021). Generation Of Digital Terrain Model from Multispectral Lidar Using Different Ground Filtering Techniques. The Egyptian Journal of Remote Sensing and Space Science, 24(2), 181-189.

[6] Morsy, S., Shaker, A., & El-Rabbany, A. (2018). Using Multispectral Airborne Lidar Data for Land/Water Discrimination: A Case Study at Lake Ontario, Canada. Applied Sciences, 8(3), 349.

[7] Zhao, P., Guan, H., Li, D., Yu, Y., Wang, H., Gao, K., ... & Li, J. (2021). Airborne Multispectral Lidar Point Cloud Classification with a Feature Reasoning-Based Graph Convolution Network. International Journal of Applied Earth Observation and Geoinformation, 105, 102634.

[8] Morsy, S., Shaker, A., & El-Rabbany, A. (2017). Multispectral Lidar Data for Land Cover Classification of Urban Areas. Sensors, 17(5), 958.

[9] Haithcoat, T. L., Song, W., & Hipple, J. D. (2001). Building Footprint Extraction and 3-D Reconstruction from Lidar Data. In IEEE/ISPRS Joint Workshop on Remote Sensing and Data Fusion over Urban Areas (Cat. No. 01EX482) (pp. 74-78). IEEE.

[10] Wang, C., Shu, Q., Wang, X., Guo, B., Liu, P., & Li, Q. (2019). A random forest classifier based on pixel comparison features for urban Lidar data. ISPRS journal of photogrammetry and remote sensing, 148, 75-86.

[11] Pan, S., Guan, H., Yu, Y., Li, J., and Peng, D. (2019). A comparative land-cover classification feature study of learning algorithms: DBM, PCA, and RF using multispectral Lidar data. IEEE Journal of Selected Topics in Applied Earth Observations and Remote Sensing 12, 1314-1326.

[12] Xiaoliang, Z., Guihua, Z., Jonathan, L., Yuanxi, Y., and Yong, F. (2016). 3D land cover classification based on multispectral lidar point clouds. International Archives of the Photogrammetry, Remote Sensing & Spatial Information Sciences 41.

[13] Ekhtari, N., Glennie, C., and Fernandez-Diaz, J. C. (2017). Classification of multispectral Lidar point clouds. In "2017 IEEE International Geoscience and Remote Sensing Symposium (IGARSS)", pp. 2756-2759. IEEE.

[14] Matikainen, L., Karila, K., Litkey, P., Ahokas, E., and Hyyppa, J. (2020). Combining single photon and multispectral airborne laser scanning for land cover classification. ISPRS Journal of Photogrammetry and Remote Sensing 164, 200-216.

[15] Yu, Y., Guan, H., Li, D., Gu, T., Wang, L., Ma, L., and Li, J. (2019). A hybrid capsule network for land cover classification using multispectral Lidar data. IEEE Geoscience and Remote Sensing Letters 17, 1263-1267.

[16] Hui, Z., Li, Z., Cheng, P., Ziggah, Y. Y., & Fan, J. (2021). Building Extraction from Airborne Lidar Data Based on Multi-Constraints Graph Segmentation. Remote Sensing, 13(18), 3766.

[17] Maltezos, E., Doulamis, A., Doulamis, N., & Ioannidis, C. (2018). Building Extraction from Lidar Data Applying Deep Convolutional Neural Networks. IEEE Geoscience and Remote Sensing Letters, 16(1), 155-159.

[18] Davydova, K., Cui, S., & Reinartz, P. (2016). Building Footprint Extraction from Digital Surface Models Using Neural Networks. In Image and Signal Processing for Remote Sensing XXII (Vol. 10004, pp. 187-196). SPIE.

[19] Nahhas, F. H., Shafri, H. Z., Sameen, M. I., Pradhan, B., & Mansor, S. (2018). Deep Learning Approach for Building Detection Using Lidar–Orthophoto Fusion. Journal of Sensors, 2018.

[20] Kaplan, G., Comert, R., Kaplan, O., Matci, D. K., & Avdan, U. (2022). Using Machine Learning to Extract Building Inventory Information Based on Lidar Data. ISPRS International Journal of Geo-Information, 11(10), 517.

[21] Zhang, P., He, H., Wang, Y., Liu, Y., Lin, H., Guo, L., & Yang, W. (2022). 3D Urban Buildings Extraction Based on Airborne Lidar and Photogrammetric Point Cloud Fusion According to U-Net Deep Learning Model Segmentation. IEEE Access, 10, 20889-20897.

[22] Brodu, N., & Lague, D. (2012). 3D Terrestrial Lidar Data Classification of Complex Natural Scenes Using a Multi-Scale Dimensionality Criterion: Applications in Geomorphology. ISPRS journal of photogrammetry and remote sensing, 68, 121-134.

[23] Optech Titan. (2018). Multispectral Lidar System Retrieved from https://geo3d.hr/sites/default/files/2018-06/Titan-Specsheet-150515-WEB.pdf

[24] Teledyne Optech Titan. (2015). Multispectral Lidar system: High Precision Environmental Mapping, Retrieved from http://www.TeledyneOptech.com/Wp-Content/Uploads/Titan- Specsheet-150515-WEB.pdf.

[25] Carrilho, A. C., Galo, M., & Santos, R. C. (2018). Statistical outlier detection method for airborne Lidar data. The International Archives of the Photogrammetry, Remote Sensing and Spatial Information Sciences, 42, 87-92.

[26] Zhang, W., Qi, J., Wan, P., Wang, H., Xie, D., Wang, X., & Yan, G. (2016). An easy-to-use airborne Lidar data filtering method based on cloth simulation. Remote sensing, 8(6), 501.